Secondary Voltage Control for Reactive Power Sharing in an Islanded Microgrid

Qian Guo[*], Hongyan Wu[*], Liaoyuan Lin[*], Zhihong Bai[*], and Hao Ma[†]

[*],[†]College of Electrical Engineering, Zhejiang University, Hangzhou, China

Abstract

Owing to mismatched feeder impedances in an islanded microgrid, the conventional droop control method typically results in errors in reactive power sharing among distributed generation (DG) units. In this study, an improved droop control strategy based on secondary voltage control is proposed to enhance the reactive power sharing accuracy in an islanded microgrid. In a DG local controller, an integral term is introduced into the voltage droop function, in which the voltage compensation signal from the secondary voltage control is utilized as the common reactive power reference for each DG unit. Therefore, accurate reactive power sharing can be realized without any power information exchange among DG units or between DG units and the central controller. Meanwhile, the voltage deviation in the microgrid common bus is removed. Communication in the proposed strategy is simple to implement because the information of the voltage compensation signal is broadcasted from the central controller to each DG unit. The reactive power sharing accuracy is also not sensitive to time-delay mismatch in the communication channels. Simulation and experimental results are provided to validate the effectiveness of the proposed method.

Key words: Droop control, Microgrid, Reactive power sharing, Secondary voltage control

I. INTRODUCTION

With the exhaustion of traditional fossil resources, distributed energy resources (DERs), such as solar arrays, fuel cells, and wind turbines, have recently attracted considerable attention. Distributed generation (DG) units integrate various types of DERs into networks with power electronic converters serving as interface devices. The concept of microgrid emerges to overcome the problem introduced by the high penetration of DG units [1], [2]. Microgrid is a small-scale power system with a localized cluster of DG units and loads. This power system coordinates multiple DG units and offers flexible operation modes unlike the conventional power system. Microgrid also provides superior power management and improves the quality of power delivered to customers.

A microgrid can operate in a grid-connected mode or an islanded mode. In the islanded mode, the microgrid is isolated from the main grid, and the total load is shared among DG units. Frequency and voltage amplitude droop control techniques are widely adopted to achieve proper load sharing [3], [4]. Droop control method provides a decentralized control capability that realizes "plug-and-play" interfacing. However, the conventional droop control method is subjected to inherent limitations of power sharing. Although real power–frequency droop (P–f droop) can share real power accurately, reactive power sharing with reactive power–voltage amplitude droop (Q–V droop) is sensitive to DG output impedance and transmission line impedance [5]–[7]. In practical microgrids, feeders may have both non-trivial inductive and resistive components. The different distances among DG units lead to mismatch in the physical impedance of the feeders, thereby resulting in significant reactive power circulation [7].

Several control techniques have been proposed recently to address the power sharing issue. A comprehensive approach is the virtual impedance concept. The dominant virtual impedance is placed at the output terminal of each DG unit to reduce the mismatch in the closed-loop output impedance. Different types of virtual impedance, such as virtual inductor [8], [9], resistor [10], and capacitor [11], are explored. However, the relevant literature has considered only output impedance. In the presence of mismatched non-negligible

feeders, an enhanced virtual impedance control scheme is investigated in [12], and the corresponding online or offline feeder impedance estimation is necessary. A $Q - \dot{V}$ droop method is proposed in [13]. The power sharing performance is improved; however, the restoration mechanism results in sharing errors. The robust droop controller proposed in [14], [15] implements an integral term using additional common bus voltage measurement for accurate power sharing and voltage drop reduction.

Communication can be adopted to enhance the reactive power sharing performance. A master–slave networked control scheme with a weighted power function formulated in the slave inverter improves power sharing accuracy [16]. However, this control scheme cannot eliminate sharing errors. In [7], the reactive power references obtained from the central energy management system are used to tune the adaptive virtual impedance, which can compensate for the mismatch in voltage drops across feeders. The method proposed in [17] utilizes low-bandwidth synchronization flag signals to activate a compensation stage for both real and reactive power sharing. A similar approach adjusts the virtual impedance [18]. The underlying assumption of these schemes is that the real power demand is constant during the compensation stage. An improved droop method activated by a sequence of synchronization signal shows enhanced sharing accuracy, but it is not robust to communication failure [19].

A hierarchical control scheme, which consists of primary, secondary, and tertiary control levels, generally standardizes the operation of microgrids [4], [20]. The primary control level deals with local control of DG units in a decentralized way. The secondary control is implemented to remove the voltage frequency and amplitude deviations inside a microgrid. Additional functions are included in the secondary control [21]–[23]. A centralized secondary control with reactive power sharing is proposed in [22], [23]. DG units transmit their output reactive power and droop coefficients to the central controller via communication. The central controller then determines the amount of reactive power for each DG unit. In the distributed secondary control scheme, each DG unit sends the measured reactive power to other DG units to be averaged, which requires a proper communication scheduling algorithm [24], [25].

Enlightened by the hierarchical control in microgrids, we propose an improved droop control strategy based on secondary voltage control in this study. The proposed strategy has two functions, namely, accurate reactive power sharing and microgrid common bus voltage restoration. On the one hand, the common bus voltage amplitude deviation is compensated for by secondary voltage control. On the other hand, the accurate reactive power sharing is achieved in the primary control level with an integral control term. This function manipulates the locally measured reactive power and the common bus voltage compensation signal from the
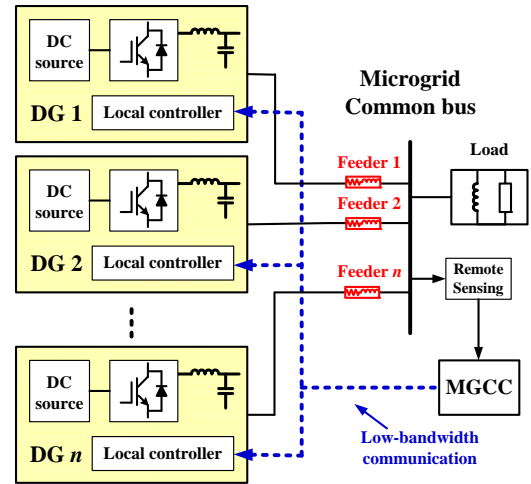

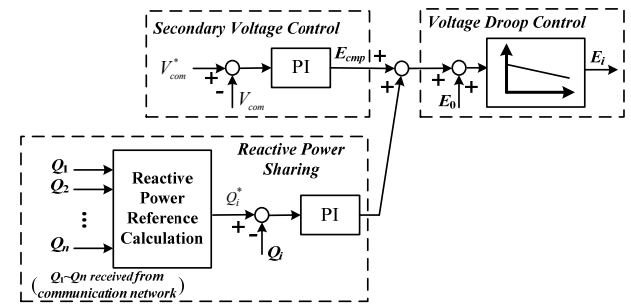Fig. 1. Islanded microgrid with a hierarchical control scheme.

Fig. 2. Conventional secondary voltage control with reactive power sharing.

secondary control. The algorithm is straightforward and easy to implement. Only one-way data links are required in the proposed scheme. The proposed method is not sensitive to the time-delay mismatch in the communication channels, and it is robust in the presence of communication failure. Simulation and experimental results indicate that the proposed method can ensure accurate reactive power sharing and improve microgrid common bus voltage.

II. ANALYSIS OF THE HIERARCHICAL CONTROL SCHEME FOR MICROGRIDS

The general configuration of an islanded microgrid with the hierarchical control scheme is shown in Fig. 1. Each DG unit consists of an energy source, an inverter, and a local controller, and is connected to the microgrid common bus through a feeder. The feeder impedance is composed of isolation transformer impedance and transmission cable impedance. According to the hierarchical control scheme [3], [4], the primary control works in a decentralized manner based on the autonomous operation of each DG local controller. The centralized secondary control loop is implemented in the microgrid central controller (MGCC), which measures the microgrid status by a remote sensing block. The MGCC generates compensation signals and sends
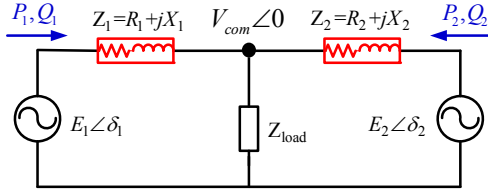
Fig. 3. Equivalent model of two DG units connected in parallel.

these signals to the primary control in each DG unit through a communication network.

A. Primary and Secondary Control

The primary control of power-electronic-based microgrids deals with local control of DG units. The technique involves microgrid voltage and frequency support, power production, and fast load tracking. The primary control generally includes voltage and current control loops, virtual impedance loop, and droop control loop. The droop control is responsible for real and reactive power management by adjusting the phase angle and the amplitude of the voltage reference. This control mimics the behavior of a synchronous generator and allows multiple DG units operate in parallel. The conventional droop control equations are expressed as

$$\omega_i = \omega_0 - m_{pi} P_i , \tag{1}$$

$$E_i = E_0 - n_{qi} Q_i , \tag{2}$$

where ω_0 and E_0 represent the rated values of DG angular frequency and voltage amplitude, respectively. ω_i and E_i are the angular frequency and the voltage amplitude references of the i-th DG unit, respectively. P_i and Q_i are the measured real and reactive powers after a low-pass filter (LPF), respectively. m_{pi} and n_{qi} represent the real and the reactive power droop coefficients, respectively.

However, the droop characteristics of the primary control have a drawback that the voltage frequency and the amplitude inside the microgrid are deviated from their nominal values. The secondary control is often employed to compensate for these deviations. The technique includes slow control loops in the MGCC, and the control output information is transmitted to each DG unit via a low-bandwidth communication system. In the secondary voltage control, as shown in Fig. 2, the root-mean-square (RMS) value of the microgrid common bus voltage V_{com} is measured and compared with the reference V_{com}^*. A slow proportional–integral (PI) controller will eliminate the voltage amplitude error and produce the amplitude restoration compensation signal E_{cmp}, which is written as follows:

$$E_{cmp} = k_{pV} \left(V_{com}^* - V_{com} \right) + k_{iV} \int \left(V_{com}^* - V_{com} \right) dt , \tag{3}$$

where k_{pV} and k_{iV} are the PI controller parameters of the secondary voltage control. The compensation signal E_{cmp} is broadcasted to the local controller of each DG unit in the microgrid. In the primary control level, E_{cmp} is added to the rated voltage E_0 in Equ. (2) to shift up the Q–V droop response

by changing the DG no-load voltage from E_0 to $E_0 + E_{cmp}$. Hence, the steady-state error can be removed. A similar procedure can be implemented for frequency restoration. Given that the primary control can perform autonomously at each DG unit with the locally measured variables, the transmission of compensation signal requires low-bandwidth communication only.

B. Reactive Power Sharing Analysis

In the steady state, all the paralleled DG units in the system operate at the same frequency, thereby guaranteeing accurate real power sharing. However, reactive power sharing is significantly affected by different DG output voltages because voltage is not a global variable.

Without loss of generality, an equivalent circuit model of an islanded microgrid with two paralleled DG units is shown in Fig. 3. $E_i \angle \delta_i$ is the output voltage of the i-th DG unit, and $V_{com} \angle 0$ is the microgrid common bus voltage. Z_i consists of the i-th DG output impedance and the feeder impedance, where R_i and X_i represent the resistance and the reactance, respectively. In this study, the analysis focuses on the fundamental real and reactive power sharing, and the harmonic power sharing issue is not considered.

The power flow together with either physical or virtual impedance causes a voltage drop, which can be approximated as [26]

$$\Delta V_i \approx \frac{X_i Q_i + R_i P_i}{E_0} . \tag{4}$$

DG voltages can be obtained from the common bus voltage by voltage drop approximation. Hence, the voltage difference in the two DG units can be expressed as

$$\Delta E = E_1 - E_2 = \left(V_{com} + \Delta V_1 \right) - \left(V_{com} + \Delta V_2 \right)$$

$$= \frac{\left(\frac{X_2}{n_{q2}} - \frac{X_1}{n_{q1}} \right) \left(n_{q1} Q_1 + n_{q2} Q_2 \right) + \left(\frac{R_2}{m_{p2}} - \frac{R_1}{m_{p1}} \right) \left(m_{p1} P_1 + m_{p2} P_2 \right)}{\frac{X_1}{n_{q1}} + \frac{X_2}{n_{q2}} + 2E_0} . \tag{5}$$

Considering Equ. (2), for the DG units to share the load in inverse proportion to their droop coefficients, their voltage amplitude difference ΔE should be zero. According to Equ. (5), ΔE equals zero if the impedances satisfy the following condition:

$$\frac{X_1}{n_{q1}} = \frac{X_2}{n_{q2}} , \frac{R_1}{m_{p1}} = \frac{R_2}{m_{p2}} . \tag{6}$$

In other words, accurate reactive power sharing is achieved if Equ. (6) holds. Therefore, the reactive power sharing among DG units depends on impedances. Reactive power is difficult to precisely share with the conventional Q–V droop control because the feeder impedances are generally mismatched in practical microgrids.

In a hierarchically controlled microgrid, reactive power

Fig. 4. Block diagram of the proposed reactive power sharing strategy based on secondary voltage control.

sharing can be achieved by adding an additional reactive power control loop in the secondary control level [22]-[25], as shown in Fig. 2. The information of the injected reactive power of each DG unit is used to decide the respective reactive power demand for each DG unit. A PI controller eliminates the reactive power sharing error by providing an additional change in the voltage amplitude of each DG unit. The PI controller can be implemented either in the MGCC or in the DG local controller. In this solution, the reactive power information of all DG units is required to transmit through the communication network, which needs a complex communication system with bidirectional messages. As in [22], DG units send the value of their output reactive power to the MGCC, and the MGCC sends back the scaled reactive power demand to each DG unit. In this way, the advantage of a centralized architecture is lost because only one-way data links are required in centralized secondary control [24].

III. PROPOSED REACTIVE POWER SHARING STRATEGY

A. Proposed Control Strategy

An improved voltage droop control method based on secondary voltage control for islanded microgrids is proposed in this study. Considering that the reactive power flow can be regulated by the voltage amplitude, the functions of reactive power sharing and voltage amplitude restoration are integrated in the proposed strategy. Hence, the proposed strategy enhances the accuracy of reactive power sharing without increasing the amount of information transmitted through the communication system.

The proposed voltage droop control method is implemented in each DG local controller, which can be expressed as

$$E_i = E_0 - n_{qi}Q_i + k_E \int \left(E_{cmp} - n_{qi}Q_i \right) dt , \qquad (7)$$

where E_{cmp} is the voltage compensation signal provided by secondary voltage control. k_E is the integral gain that regulates the dynamic response of the controller. A comparison between Equs. (7) and (2) indicates that the integral term in Equ. (7) will manipulate the common bus voltage compensation signal E_{cmp} together with the locally measured reactive power of each DG unit. The real power control is based on Equ. (1).

The control block diagram of the proposed strategy based on secondary voltage control is shown in Fig. 4. The proposed strategy does not change the original secondary voltage control. The MGCC measures the microgrid common bus voltage and calculates its RMS value. The voltage compensation signal E_{cmp} is generated by a slow PI controller in accordance with Equ. (3) and broadcasted to each DG unit via low-bandwidth communication. The DG local controller adopts the proposed voltage droop control method in accordance with Equ. (7).

In a stable system, the input of the integral term in Equ. (7) should be zero in the steady state. Thus,

$$n_{qi}Q_i = E_{cmp} . \qquad (8)$$

When the voltage compensation signal E_{cmp} is broadcasted by the MGCC to all the DG units in the microgrid, all DG units receive the same value of E_{cmp}. Compared with the conventional secondary voltage control, in which the compensation signal E_{cmp} is added to the nominal value E_0 in the primary level, E_{cmp} works as a common reference for the reactive power of each DG unit in the proposed method. Therefore, $n_{q1}Q_1 = n_{q2}Q_2 = \ldots = n_{qn}Q_n$, and the reactive power is

shared in inverse proportion to the voltage droop coefficients. The effect of impedance mismatch on the reactive power sharing can be eliminated without acquiring knowledge of the feeder impedances. The integral term generates different output voltages for different DG units, which compensate for the unequal voltage drops across the mismatched impedances.

Meanwhile, the function of secondary voltage control for compensating for the voltage amplitude deviation is not affected. The input of the integral term in Equ. (3) also equals zero in the steady state. Therefore, the microgrid common bus voltage can be restored to its nominal value with $V_{com}{=}V_{com}^*$.

In the proposed strategy, the communication system is simple to implement. The information transmitted through the communication channel is only the voltage compensation signal E_{cmp}, which is the same as that of the original secondary voltage control. E_{cmp} is also broadcasted from the MGCC to each DG unit. In contrast to the conventional reactive power control loop implemented in secondary control, the reactive power information exchange among DG units or between DG units and the MGCC is no longer necessary in the proposed scheme. Hence, the communication is not too busy, and network congestion can be avoided. One-way data links are adequate for the communication network of the proposed scheme, which will not increase the complexity of the communication system for the original secondary voltage control.

Intrinsic transmission delays exist in practical communication networks. Nonetheless, the proposed strategy remains effective in the presence of time-delay mismatch among the communication links of different DG units. In the steady state, microgrid common bus voltage is regulated to its nominal value. The voltage compensation signal E_{cmp}, which is the output of secondary control, is not time variant. The same value of E_{cmp} for all DG units can be assured. Therefore, the proposed strategy is robust to time-delay mismatch. However, the system will experience a different transient response in contrast to that with the same time delay in the communication channels.

B. Small-signal state-space modeling and analysis

A small-signal state-space model is derived for the proposed strategy based on the modeling method in [27]. The physical configuration of the microgrid system is formulated, which consists of DG units, a distribution network, and loads. Considering a three-phase islanded microgrid with n DG units, the relationship between DG output current vector $I = [\vec{I}_1, \vec{I}_2, \cdots, \vec{I}_n]^\text{T}$ and output voltage vector $E = [\vec{E}_1, \vec{E}_2, \cdots, \vec{E}_n]^\text{T}$ is written as

$$I=YE , \tag{9}$$

where $Y = [Y_{ij}]$ represents the reduced system admittance matrix by Kron reduction. The non-generating nodes are removed from the node voltage equations. The element Y_{ij} can be written as a rectangular form $Y_{ij}= G_{ij} + jB_{ij}$. Given that the

complex power injected by the i-th DG unit is $s_i = 3\vec{E}_i\vec{I}_i^*$, the instantaneous real and reactive powers can be expressed as

$$p_i = 3E_i\sum_{j=1}^{n}E_j\left(G_{ij}\cos(\delta_i - \delta_j)+B_{ij}\sin(\delta_i - \delta_j)\right), \tag{10}$$

$$q_i = 3E_i\sum_{j=1}^{n}E_j\left(G_{ij}\sin(\delta_i - \delta_j)-B_{ij}\cos(\delta_i - \delta_j)\right), \tag{11}$$

where δ_i refers to the relative phase angle between the i-th DG unit and the microgrid common bus. Around the system equilibrium point, linearizing Equs. (10) and (11) obtains

$$\Delta p_i = \sum_{j=1}^{n}\left(\frac{\partial p_i}{\partial \delta_j}\Delta\delta_j + \frac{\partial p_i}{\partial E_j}\Delta E_j\right), \tag{12}$$

$$\Delta q_i = \sum_{j=1}^{n}\left(\frac{\partial q_i}{\partial \delta_j}\Delta\delta_j + \frac{\partial q_i}{\partial E_j}\Delta E_j\right). \tag{13}$$

The DG units are regarded as controllable voltage sources to focus on the dynamic performance of power control. Only the power sharing control method with low-frequency dominant modes is studied in the modeling process. Therefore, the linearized equations of Equs. (1) and (7) are expressed as

$$\Delta\dot{\delta}_i{=}-m_{pi}\Delta P_i , \tag{14}$$

$$\Delta\dot{E}_i{=}-n_{qi}\Delta\dot{Q}_i{+}k_E\left(\Delta E_{cmp}-n_{qi}\Delta Q_i\right). \tag{15}$$

The average real and reactive powers are obtained through first-order LPF with the bandwidth ω_c as

$$\Delta P_i{=}\frac{\omega_c}{s + \omega_c}\Delta p_i , \quad \Delta Q_i{=}\frac{\omega_c}{s + \omega_c}\Delta q_i . \tag{16}$$

The dynamic performance of the secondary voltage controller is considered. Linearizing Equ. (3) obtains

$$\Delta E_{cmp}{=}-\left(k_{pV}\Delta V_{com}{+}k_{iV}\Delta\gamma\right), \tag{17}$$

where the integrator state $\Delta\gamma$ is defined as $\Delta\dot{\gamma}{=}\Delta V_{com}$.

The microgrid common bus voltage phasor $\vec{V}_{com}{=}V_{com}\angle 0$ can be presented as a linear combination of DG output voltage phasors shown as

$$\vec{V}_{com} = c_1\vec{E}_1 + c_2\vec{E}_2 + \cdots + c_n\vec{E}_n , \tag{18}$$

where $c = [c_1, c_2, \ldots, c_n]$ is a set of scalars. Each element of c is a constant, and its value can be calculated from node voltage equations, which are based on microgrid physical configuration.

On the basis of Equ. (18) and considering $\vec{E}_i{=}E_i\angle\delta_i$, the linearized expression for ΔV_{com} can be obtained as

$$\Delta V_{com}{=}\sum_{j=1}^{n}\left(\frac{\partial V_{com}}{\partial\delta_j}\Delta\delta_j + \frac{\partial V_{com}}{\partial E_j}\Delta E_j\right). \tag{19}$$

The linearized equations presented in Equs. (12)–(17) and (19) can be combined to construct the small-signal state-space model of the microgrid system with the proposed control strategy. The complete model can be written in a compact form shown as

TABLE I

SYSTEM PARAMETERS

	Parameters		Values
Electrical Setup	rated microgrid frequency		50 Hz
	rated microgrid voltage (line-line)	simulation	380 V
		experiment	190 V
	total load	simulation	7.05 kW, 6.75 kvar
		experiment	2 kW, 0.5 kvar
	inverter filter (L_f, C_f)		6 mH, 2 μF
	switching frequency (f_s)		10 kHz
Control Parameters — Primary	LPF bandwidth (ω_c)		$2\pi \times 10$ rad/s
	frequency droop coefficient (m_p)	simulation	2×10^{-4} rad/(s·W)
		experiment	2×10^{-4} rad/(s·W)
	voltage droop coefficient (n_q)	simulation	2.5×10^{-3} V/var
		experiment	2×10^{-3} V/var
	integral gain (k_E)	simulation	15 s^{-1}
		experiment	2 s^{-1}
Control Parameters — Secondary	proportional term (k_{pV})	simulation	0.5
		experiment	2
	integral term (k_{iV})	simulation	2 s^{-1}
		experiment	1 s^{-1}

$$\dot{\boldsymbol{x}}_{MG}(t) = \boldsymbol{A}_{MG}\boldsymbol{x}_{MG}(t), \qquad (20)$$

where the state vector is $\boldsymbol{x}_{MG} = [\Delta\delta_1, \Delta\delta_2, \ldots, \Delta\delta_n, \Delta P_1, \Delta P_2, \ldots, \Delta P_n, \Delta Q_1, \Delta Q_2, \ldots, \Delta Q_n, \Delta E_1, \Delta E_2, \ldots, \Delta E_n, \Delta\gamma]^T$, which contains $4n + 1$ state variables. The detailed expression of $\boldsymbol{A}_{MG}$ can be extracted from Equs. (12)–(19), and it is shown in the Appendix.

An islanded microgrid system with three identical DG units is investigated to evaluate the proposed scheme. The system parameters are listed in Table I and are the same as the simulation parameters. In the microgrid system shown in Fig. 1, each DG unit is connected to the microgrid common bus through a feeder. The feeder impedances of the DG units are set as $Z_{l1} = 0.2 + j0.3$ Ω, $Z_{l2} = 0.5 + j0.6$ Ω, and $Z_{l3} = 0.3 + j0.38$ Ω to emphasize the discrepancy in the impedances. The load connected to the common bus is described as a lump load Z_L. The DG units are intended to share the load equally.

The root locus diagram with the variation in the integral gain k_E is shown in Fig. 5. k_E is initially assumed to be zero, and the proposed method is reduced to the conventional droop control. The associated poles are denoted by "o." Zero eigenvalue λ_1 is the consequence of the independent DG unit angles. Other zero eigenvalues λ_2–λ_5 are related to the integral term and the secondary control. Two pairs of complex conjugate poles λ_6–λ_9 are shaped by the power droop control. The remaining eigenvalues λ_{10}–λ_{13} are located on the far left of the s-plane, which are neglected in Fig. 5. As k_E increases, a high damping ratio is provided for secondary control. The eigenvalues λ_4 and λ_5 move further left along the real axis, and λ_2 and λ_3 becomes a pair of complex poles. These dominant eigenvalues are shifted to offer a good dynamic response by adjusting k_E. However, the eigenvalues λ_6–λ_9 associated with power droop control are also
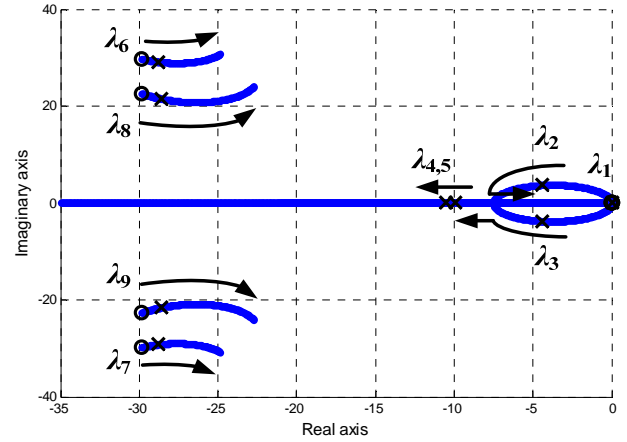
Fig. 5. Root locus diagram of the proposed scheme with variation in integral gain k_E. ($0 \leq k_E \leq 50$).

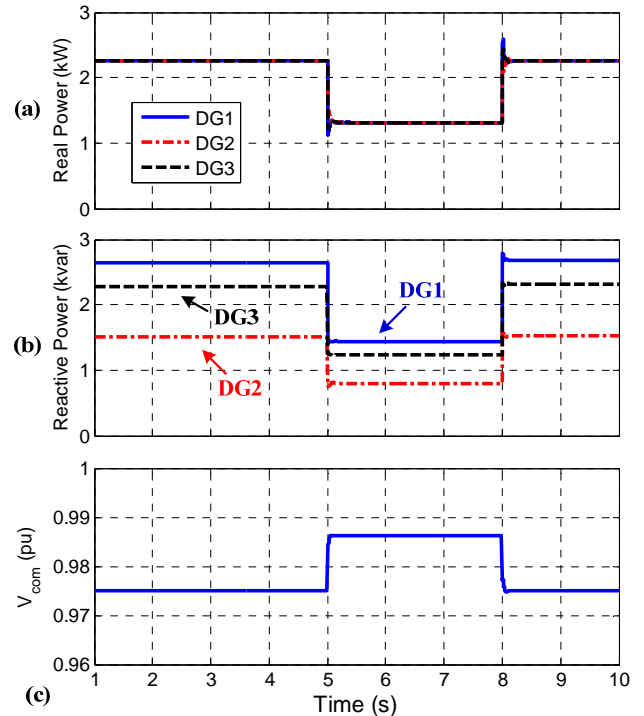Fig. 6. Simulated performance of the conventional droop control scheme (a) real power, (b) reactive power, and (c) common bus voltage.

influenced by k_E. With increasing k_E, they gradually become underdamped, thereby leading to a more oscillatory response for primary droop control. The desired eigenvalues are marked by "x" with the integral gain $k_E = 15$.

IV. SIMULATION AND EXPERIMENTAL RESULTS

A. Simulation Verification

The islanded microgrid model discussed in Section III is simulated in the MATLAB/Simulink environment to validate the proposed control strategy. The P-ω droop is implemented for real power regulation. The secondary voltage controller broadcasts the common bus voltage compensation signal E_{cmp}
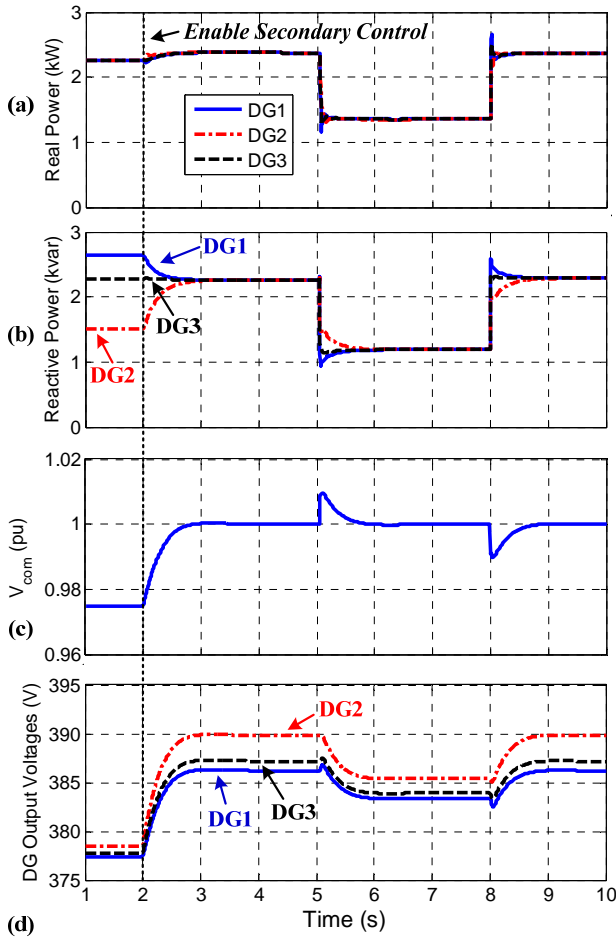
Fig. 7. Simulated performance of the proposed control strategy (a) real power, (b) reactive power, (c) common bus voltage, and (d) DG local output voltages.
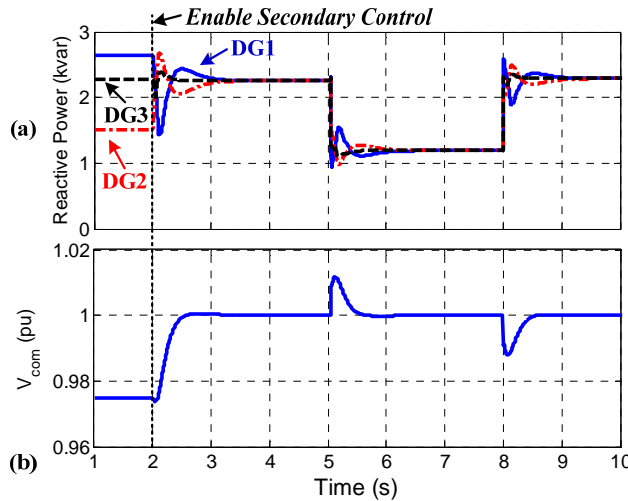

Fig. 8. Simulated performance of the proposed control strategy in the presence of time-delay mismatch in the communication channels (a) reactive power and (b) common bus voltage.

to each DG unit in every line period.

Fig. 6 demonstrates the system performance with the conventional droop control scheme. The total reactive power load is changed between 6.75 and 3.6 kvar at $t = 5$ s and $t = 8$ s,

whereas the real power load is changed between 7.05 and 4.05 kW. Although the real power is shared equally, significant errors exist in the reactive power sharing because of the mismatched feeders. The droop characteristics of the power control and voltage drop across the impedances result in common bus voltage deviation.

The same procedure is conducted with the proposed strategy. The results are illustrated in Fig. 7. The secondary voltage control is activated at $t = 1$ s. The reactive power sharing error is reduced to zero in approximately 1 s. Only a small transient effect occurs on the real power when the proposed control strategy is enabled. The common bus voltage is gradually restored to 1 p.u., and the voltage static deviation is eliminated. The DG local output voltages are obtained in Fig. 7(d). These voltages are shifted up slightly because of the integral term in Equ. (7). The DG output voltages are different to compensate for the unequal voltage drops across the mismatched impedances. For instance, DG unit 2 with a large feeder impedance injects minimal reactive power with the conventional droop control. After the start of the secondary control, the integral term generates a higher voltage amplitude for DG unit 2 to remove the effect of its feeder. Hence, equal reactive power sharing and common bus voltage restoration are realized.

The simulated performance of the proposed method in the presence of communication delay mismatch among the communication channels is demonstrated in Fig. 8. To emphasize the time-delay mismatch, different delay times (0.1 and 0.05 s) are intentionally added to the communication channels of DG units 1 and 3, whereas no delay time is set for DG unit 2. The communication delay mismatch has no effect on the power sharing accuracy in the proposed method. The common bus voltage shows no steady-state error. Compared with the results shown in Fig. 7, only dynamic performance is influenced.

B. Experimental Verification

An islanded microgrid prototype with two identical DG units is constructed to verify the proposed control strategy. Each DG unit is based on a three-phase inverter using a Mitsubishi PM50RL1A120 intelligent power module and controlled by a TMS320F28335 digital signal processor (DSP). Two DG units are intended to achieve 1:1 power sharing. The experimental system parameters are listed in Table I. Each DG unit is connected to the microgrid common bus through a Δ-Y isolation transformer with 1 mH leakage inductance and 0.2 Ω resistance. The mismatched feeder impedances are constructed by adding 0.5 Ω resistor in the feeder of DG unit 2. A third DSP control board equipped with microgrid common bus measurement is employed as the MGCC, which operates the centralized secondary voltage control loop. The RMS value of the common bus voltage passes through a low-pass prefilter with 100 Hz cutoff frequency before it is used in the secondary
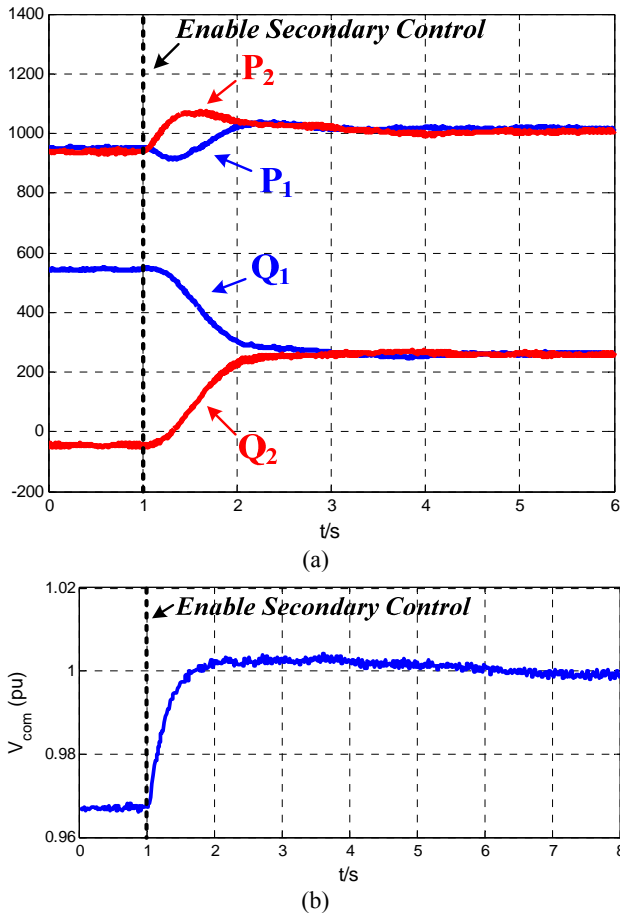
Fig. 9. Experimental performance of the proposed controller (a) real power (200 W/div) and reactive power (200 var/div) and (b) common bus voltage.
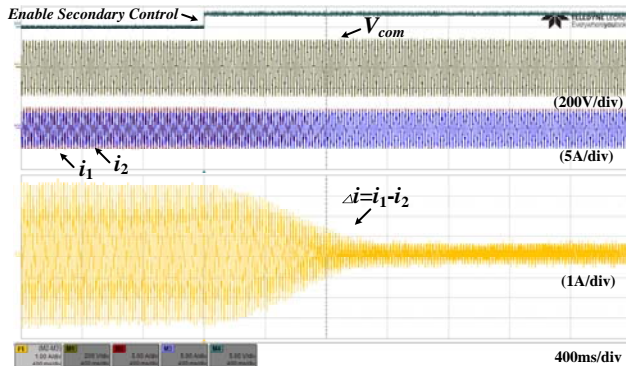

Fig. 10. Compensation process of the proposed controller.

control. Given the configuration of the hardware system, a controller area network bus is utilized for the communication network, but the proposed control strategy is not constrained to this communication method. The microgrid common bus voltage compensation signal is broadcasted from the MGCC to each DG unit in every line period.

The experimental performance of the proposed strategy is depicted in Fig. 9. The real power and reactive power are internally measured in the controller and recorded in a computer that runs the data acquisition system. The DG units
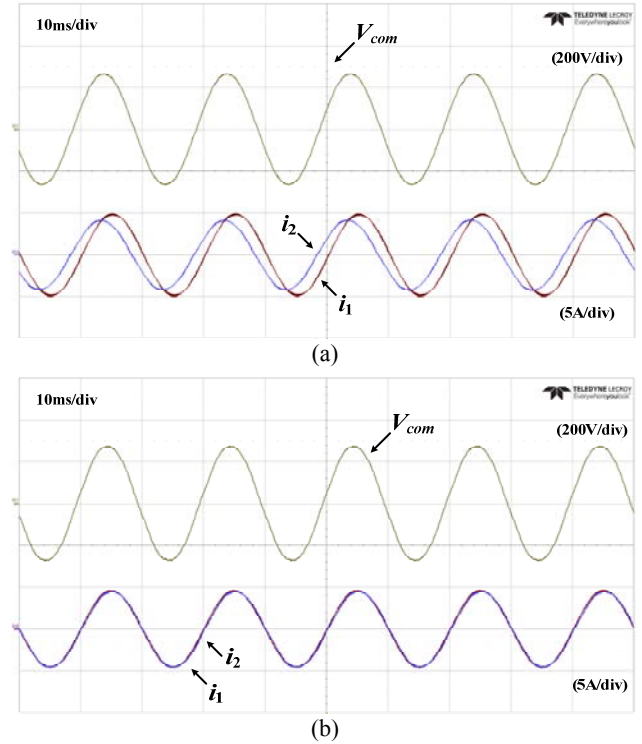
Fig. 11. Steady-state experimental waveforms (a) with the conventional droop controller and (b) with the proposed controller.

initially operate under the conventional droop method.

Although the real powers can be shared equally, the mismatched feeder impedances result in poor reactive power sharing. Given that DG unit 1 has smaller impedance, it injects more reactive power. Voltage drop appears in the microgrid common bus. After the secondary voltage control starts at t = 1 s, the reactive power sharing error is gradually reduced, and equal power sharing is eventually achieved. Meanwhile, the common bus voltage is restored to its nominal value. Owing to the power coupling introduced by the complex feeder impedances, sharing errors exist in the real power during the compensation process. After the compensation process, the real power is equally shared again and is larger than the original value because the common bus voltage is increased.

The experimental waveforms associated with Fig. 9 are shown in Fig. 10. The DG output currents and the common bus voltage are regulated smoothly during the compensation process. After enabling secondary voltage control, the DG current difference $\Delta i = i_1 - i_2$ is reduced significantly. The zoomed steady-state waveforms are shown in Fig. 11. The current difference is obvious with the use of the conventional droop controller, whereas two current waveforms are almost identical with the proposed strategy.

A similar experiment is conducted in the presence of time-delay mismatch in communication channels. A 0.1 s delay is intentionally added to the communication channel of DG unit 1, whereas a 0.05 s delay is set for DG unit 2. The results
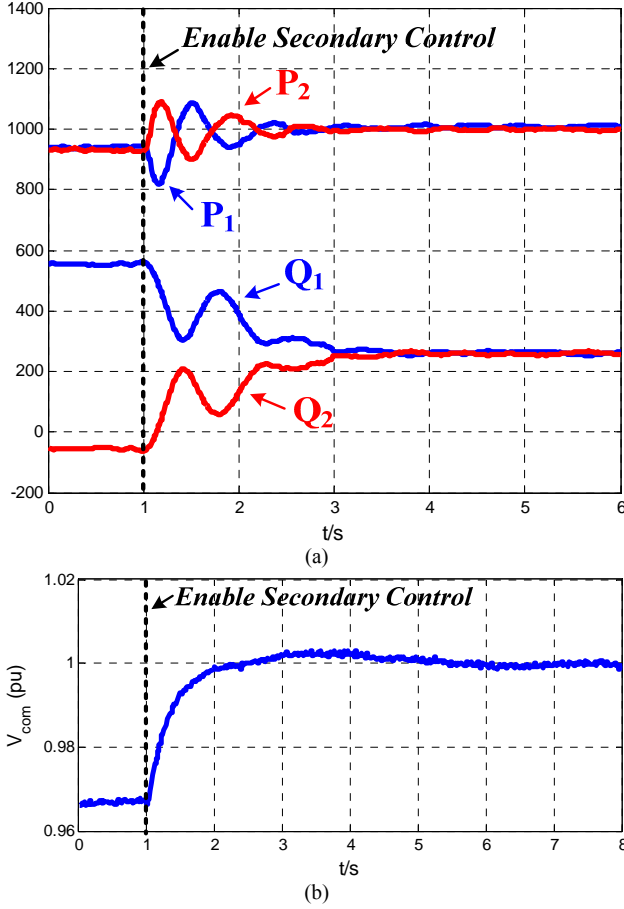
Fig. 12. Experimental performance of the proposed controller with time delay in the communication channel (a) real power (200 W/div) and reactive power (200 var/div) and (b) common bus voltage.
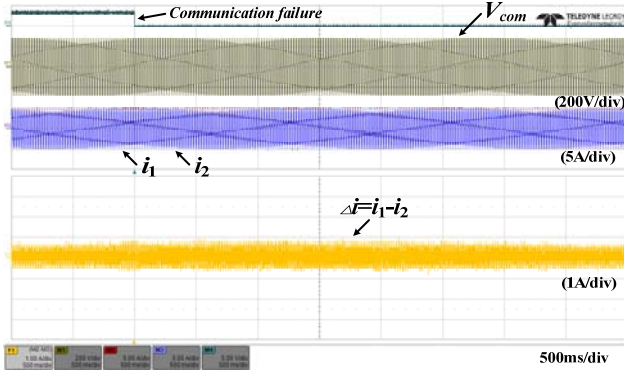

Fig. 13. Performance of the proposed controller after communication failure.

are shown in Fig. 12. The setting time of power flow is increased, and the response exhibits a damped oscillation. In comparison with the results in Fig. 9, the communication-delay mismatch affects the transient response only. Accurate power sharing is eventually achieved, and the common bus voltage deviation can be removed. Fig. 13 shows the performance of the proposed strategy when a communication failure occurs. After the secondary control is disabled, a communication timeout is detected by DG units. In the DG local controller, the integral term in Equ. (7) stops updating, and the output of integrator maintains its last value before the communication failure. The current difference in Fig. 13 remains a small value. The results in Figs. 12 and 13 indicate that the proposed strategy is robust to communication delay mismatch and communication failure.

V. CONCLUSION

In this study, an improved reactive power sharing strategy based on secondary voltage control is proposed. The method employs an integral term for DG voltage amplitude regulation in a DG local controller. In the integral term, the voltage compensation signal, which is generated by secondary voltage control, works as a common reference for each DG reactive power. Therefore, accurate reactive power sharing can be achieved in addition to microgrid common bus voltage amplitude restoration. Given that the voltage compensation signal is broadcasted from the MGCC to each DG unit, the communication system is simple with only unidirectional messages required in the proposed scheme. Power information exchange among DG units or between DG units and the central controller is not necessary. Furthermore, the proposed method is not sensitive to time-delay mismatch in communication channels, and it is robust to communication failure. The simulation and experimental results are both presented to verify the effectiveness of the proposed control strategy.

APPENDIX

The detailed expression of A_{MG} is shown in Equ. (21) at the bottom of the next page, where

$$M_p = \begin{pmatrix} -m_{p1} & \cdots & 0 \\ \vdots & \ddots & \vdots \\ 0 & \cdots & -m_{pn} \end{pmatrix}_{n \times n}, \quad N_q = \begin{pmatrix} -n_{q1} & \cdots & 0 \\ \vdots & \ddots & \vdots \\ 0 & \cdots & -n_{qn} \end{pmatrix}_{n \times n},$$

$$A_{p\delta} = \begin{pmatrix} \dfrac{\partial p_1}{\partial \delta_1} & \cdots & \dfrac{\partial p_1}{\partial \delta_n} \\ \vdots & \ddots & \vdots \\ \dfrac{\partial p_n}{\partial \delta_1} & \cdots & \dfrac{\partial p_n}{\partial \delta_n} \end{pmatrix}_{n \times n}, \quad A_{pE} = \begin{pmatrix} \dfrac{\partial p_1}{\partial E_1} & \cdots & \dfrac{\partial p_1}{\partial E_n} \\ \vdots & \ddots & \vdots \\ \dfrac{\partial p_n}{\partial E_1} & \cdots & \dfrac{\partial p_n}{\partial E_n} \end{pmatrix}_{n \times n},$$

$$A_{MG} = \begin{bmatrix} O_{n \times n} & M_p & O_{n \times n} & O_{n \times n} & O_{n \times 1} \\ \omega_c A_{p\delta} & -\omega_c I_n & O_{n \times n} & \omega_c A_{pE} & O_{n \times 1} \\ \omega_c A_{q\delta} & O_{n \times n} & -\omega_c I_n & \omega_c A_{qE} & O_{n \times 1} \\ -k_E k_{pV} \mathbf{1_n} C_{V\delta} - \omega_c B_{q\delta} & O_{n \times n} & (k_E - \omega_c) N_q & -k_E k_{pV} \mathbf{1_n} C_{VE} - \omega_c B_{qE} & -k_E k_{iV} \mathbf{1_n} \\ C_{V\delta} & O_{1 \times n} & O_{1 \times n} & C_{VE} & 0 \end{bmatrix} \quad (21)$$

$$A_{q\delta} = \begin{pmatrix} \dfrac{\partial q_1}{\partial \delta_1} & \cdots & \dfrac{\partial q_1}{\partial \delta_n} \\ \vdots & \ddots & \vdots \\ \dfrac{\partial q_n}{\partial \delta_1} & \cdots & \dfrac{\partial q_n}{\partial \delta_n} \end{pmatrix}_{n \times n}, \quad A_{qE} = \begin{pmatrix} \dfrac{\partial q_1}{\partial E_1} & \cdots & \dfrac{\partial q_1}{\partial E_n} \\ \vdots & \ddots & \vdots \\ \dfrac{\partial q_n}{\partial E_1} & \cdots & \dfrac{\partial q_n}{\partial E_n} \end{pmatrix}_{n \times n},$$

$$B_{q\delta} = \begin{pmatrix} n_{q1}\dfrac{\partial q_1}{\partial \delta_1} & \cdots & n_{q1}\dfrac{\partial q_1}{\partial \delta_n} \\ \vdots & \ddots & \vdots \\ n_{qn}\dfrac{\partial q_n}{\partial \delta_1} & \cdots & n_{qn}\dfrac{\partial q_n}{\partial \delta_n} \end{pmatrix}_{n \times n}, \quad B_{qE} = \begin{pmatrix} n_{q1}\dfrac{\partial q_1}{\partial E_1} & \cdots & n_{q1}\dfrac{\partial q_1}{\partial E_n} \\ \vdots & \ddots & \vdots \\ n_{qn}\dfrac{\partial q_n}{\partial E_1} & \cdots & n_{qn}\dfrac{\partial q_n}{\partial E_n} \end{pmatrix}_{n \times n},$$

$$C_{V\delta} = \begin{pmatrix} \dfrac{\partial V_{com}}{\partial \delta_1} & \cdots & \dfrac{\partial V_{com}}{\partial \delta_n} \end{pmatrix}_{1 \times n}, \quad C_{VE} = \begin{pmatrix} \dfrac{\partial V_{com}}{\partial E_1} & \cdots & \dfrac{\partial V_{com}}{\partial E_n} \end{pmatrix}_{1 \times n},$$

O is the zero matrix, $I_n \in R^{n \times n}$ is the identity matrix, and $1_n = [1,1,\ldots,1]^T \in R^{n \times 1}$ is a column vector.

ACKNOWLEDGMENT

REFERENCES

[1] D. E. Olivares, A. Mehrizi-Sani, A. H. Etemadi, C. A. Cañizares, and R. Palma-Behnke, "Trends in microgrid control," *IEEE Trans. Smart Grid*, Vol. 5, No. 4, pp. 1905-1919, Jul. 2014.

[2] X. Wang, J. M. Guerrero, F. Blaabjerg and Z. Chen, "A review of power electronics based microgrids," *Journal of Power Electronics*, Vol. 12, No. 1, pp. 181-192, Jan. 2012.

[3] J. Rocabert, A. Luna, F. Blaabjerg, and P. Rodríguez, "Control of power converters in AC microgrids," *IEEE Trans. Power Electron.*, Vol. 27, No. 11, pp. 4734-4749, Nov. 2012.

[4] J. M. Guerrero, J. C. Vasquez, J. Matas, L. Vicuna, and M. Castilla, "Hierarchical control of droop-controlled AC and DC microgrids: A general approach toward standardization," *IEEE Trans. Ind. Electron.*, Vol. 58, No. 1, pp. 158-172, Jan. 2011.

[5] X. Zhang, J. Liu, Z. You, and T. Liu, "Study on the influence of distribution lines to parallel inverter systems adopting the droop control method," *Journal of Power Electronics*, Vol. 13, No. 4, pp. 701-711, Jul. 2013.

[6] W. Yao, M. Chen, J. Matas, J. M. Guerrero, and Z. Qian, "Design and analysis of the droop control method for parallel inverters considering the impact of the complex impedance on the power sharing," *IEEE Trans. Ind. Electron.*, Vol. 58, No. 2, pp. 576-588, Feb. 2011.

[7] H. Mahmood, D. Michaelson, and J. Jiang, "Accurate reactive power sharing in an islanded microgrid using adaptive virtual impedances," *IEEE Trans. Power*

Electron., Vol. 30, No. 3, pp. 1605-1617, Mar. 2015.

[8] J. M. Guerrero, J. Matas, L. Vicuna, M. Castilla, and J. Miret, "Wireless-control strategy for parallel operation of distributed-generation inverters," *IEEE Trans. Ind. Electron.*, Vol. 53, No. 5, pp. 1461-1470, Oct. 2006.

[9] Z. Guo, D. Sha, and X. Liao, "Wireless paralleled control strategy of three-phase inverter modules for islanding distributed generation systems," *Journal of Power Electronics*, Vol. 13, No. 3, pp. 479-486, May 2013.

[10] J. M. Guerrero, J. Matas, L. Vicuna, M. Castilla, and J. Miret, "Decentralized control for parallel operation of distributed generation inverters using resistive output impedance," *IEEE Trans. Ind. Electron.*, Vol. 54, No. 2, pp. 994-1004, Apr. 2007.

[11] Q. Zhong and Y. Zeng, "Control of inverters via a virtual capacitor to achieve capacitive output impedance," *IEEE Trans. Power Electron.*, Vol. 29, No. 10, pp. 5568-5578, Oct. 2014.

[12] J. He, Y. W. Li, J. M. Guerrero, F. Blaabjerg, and J. C. Vasquez, "An islanding microgrid power sharing approach using enhanced virtual impedance control scheme," *IEEE Trans. Power Electron.*, Vol. 28, No. 11, pp. 5272-5282, Nov. 2013.

[13] C.-T. Lee, C.-C. Chu, and P.-T. Cheng, "A new droop control method for the autonomous operation of distributed energy resource interface converters," *IEEE Trans. Power Electron.*, Vol. 28, No. 4, pp. 1980-1993, Apr. 2013.

[14] Q. Zhong, "Robust droop controller for accurate proportional load sharing among inverters operated in parallel," *IEEE Trans. Ind. Electron.*, Vol. 60, No. 4, pp. 1281-1290, Apr. 2013.

[15] C. K. Sao and P. W. Lehn, "Autonomous load sharing of voltage source converters," *IEEE Trans. Power Del.*, Vol. 20, No. 2, pp. 1009-1016, Apr. 2005.

[16] Y. Zhang and H. Ma, "Theoretical and experimental investigation of networked control for parallel operation of inverters," *IEEE Trans. Ind. Electron.*, Vol. 59, No. 4, pp. 1961-1970, Apr. 2012.

[17] J. He and Y. W. Li, "An enhanced microgrid load demand sharing strategy," *IEEE Trans. Power Electron.*, Vol. 27, No. 9, pp. 3984-3995, Sep. 2012.

[18] J. He, Y. W. Li, and F. Blaabjerg, "An enhanced islanding microgrid reactive power, imbalance power, and harmonic power sharing scheme," *IEEE Trans. Power Electron.*, Vol. 30, No. 6, pp. 3389-3401, Jun. 2015.

[19] H. Han, Y. Liu, Y. Sun, M. Su, and J. M. Guerrero, "An improved droop control strategy for reactive power sharing in islanded microgrid," *IEEE Trans. Power Electron.*, Vol. 30, No. 6, pp. 3133-3141, Jun. 2015.

[20] A. Bidram and A. Davoudi, "Hierarchical structure of microgrids control system," *IEEE Trans. Smart Grid*, Vol. 3, No. 4, pp. 1963-1976, Dec. 2012.

[21] M. Savaghebi, A. Jalilian, J. C. Vasquez, and J. M. Guerrero, "Secondary control for voltage quality enhancement in microgrids," *IEEE Trans. Smart Grid*, Vol. 3, No. 4, pp. 1893-1902, Dec. 2012.

[22] A. Micallef, M. Apap, C. Spiteri-Staines, J. M. Guerrero, and J. C. Vasquez, "Reactive power sharing and voltage harmonic distortion compensation of droop controlled single phase islanded microgrids," *IEEE Trans. Smart Grid*, Vol. 5, No. 3, pp. 1149-1158, May 2014.

[23] A. Micallef, M. Apap, C. S. Staines, and J. M. Guerrero Zapata, "Secondary control for reactive power sharing and voltage amplitude restoration in droop-controlled islanded

microgrids," in *3rd IEEE International Symposium on Power Electronics for Distributed Generation Systems(PEDG)*, pp. 492-498, Jun. 2012.

[24] Q. Shafiee, J. M. Guerrero, and J. C. Vasquez, "Distributed secondary control for islanded microgrids – A novel approach," *IEEE Trans. Power Electron.*, Vol. 29, No. 2, pp. 1018-1031, Feb. 2014.

[25] Q. Shafiee, C. Stefanovic, T. Dragicevic, P. Popovski, J. C. Vasquez, and J. M. Guerrero, "Robust networked control scheme for distributed secondary control of islanded microgrids," *IEEE Trans. Ind. Electron.*, Vol. 61, No. 10, pp. 5363-5374, Oct. 2014.

[26] Y. W. Li and C. Kao, "An accurate power control strategy for power-electronics-interfaced distributed generation units operating in a low-voltage multibus microgrid," *IEEE Trans. Power Electron.*, Vol. 24, No. 12, pp. 2977-2988, Dec. 2009.

[27] A. Kahrobaeian and Y. A. R. I. Mohamed, "Networked-based hybrid distributed power sharing and control for islanded microgrid systems," *IEEE Trans. Power Electron.*, Vol. 30, No. 2, pp. 603-617, Feb. 2015.
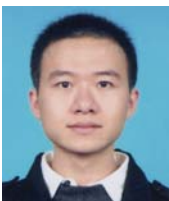
Hao Ma was born in Hangzhou, China. He received his B.S., M.S., and Ph.D. degrees in Electrical Engineering from Zhejiang University, Hangzhou, China in 1991, 1994, and 1997, respectively. He is currently a professor in the College of Electrical Engineering, Zhejiang University. His research interests include advanced control in power electronics, fault diagnosis of power electronic circuits and systems, and application of power electronics.

Qian Guo was born in Zhengzhou, China. She received her B.S. degree in Electrical Engineering from Zhejiang University, Hangzhou, China in 2010. She is currently working toward her Ph.D. degree in Electrical Engineering at the same university. Her research interests include control of inverters in microgrids and distributed generation systems.

Hongyan Wu was born in Ningbo, China. He received his B.S. degree in Electronic Information Engineering from Zhejiang University City College, Hangzhou, China in 2013. He is currently working toward his M.S. degree in Electrical Engineering at Zhejiang University, Hangzhou, China. His research interests include digital control technique and renewable energy generation system.

Liaoyuan Lin was born in Quanzhou, China. He received his B.S. degree in Electrical Engineering from Zhejiang University, Hangzhou, China in 2012. He is currently working toward his Ph.D. degree in Electrical Engineering at the same university. His research interests include parallel operation of inverters, distributed generation, and microgrids

Zhihong Bai was born in Shanxi, China. She received her Ph.D. degree in Electrical Engineering from Zhejiang University, Hangzhou, China in 2008. Since 2011, she has been with Zhejiang University, Hangzhou, China, where she is currently an associate professor in the College of Electrical Engineering. Her current research interests include renewable energy system and high-power and multilevel converters.